J. Radiat. Res., 45, 423–433 (2004)

Regular Paper

Strain Dependent Differences in a Histological Study of CD44 and Collagen Fibers with an Expression Analysis of Inflammatory Response-related Genes in Irradiated Murine Lung

Mayumi IWAKAWA*, Shuhei NODA, Toshie OHTA, Chisa OOHIRA, Hiroko TANAKA, Atsushi TSUJI, Atsuko ISHIKAWA, and Takashi IMAI

Murine strain/Radiation/Lung fibrosis/Inflammation/Gene

Using a mouse model, we investigated the mechanisms of heterogeneity in response to ionizing radiation in this research. C57BL/6J and C3H/HeMs mice were irradiated with gamma rays at 10 and 20 Gy. The animals were sacrificed at times corresponding to the latent period, the pneumonic phase, and the start of the fibrotic phase for histological investigation. Small areas of fibrosis initially appeared in C57BL/6J mice at 4 weeks postirradiation with 20 Gy, whereas small inflammatory lesions appeared at 4 and 8 weeks after 20 and 10 Gy, respectively. The alveoli septa were thickened by an infiltration of inflammatory cells, and alveoli were obliterated in lungs from C57BL/6J mice after 20 Gy irradiation. At 24 hours and from 2 to 4 weeks postirradiation, fourfold more CD44 positive cells had accumulated in the lungs of C3H/HeMs than in C57BL/6J mice. Hyaluronan accumulated 12 hours after irradiation, and the rapid resolution was achieved within 2 weeks in the lungs in both strains of mice. C57BL/6J mice lungs accumulated dense collagen at 8 weeks. Quantitative RT-PCR assay was performed for several genes selected by cDNA microarray analysis. The expression of several genes, such as Cap1, Il18, Mmp12, Per3, Ltf, Ifi202a, and Rad51ap1 showed strain-dependent variances. In conclusion, a histological investigation suggested that C3H/HeMs mice were able to induce a more rapid clearance of matrix after irradiation than C57BL/6J mice. The expression analysis showed that the several genes are potentially involved in inter-strain differences in inflammatory response causing radiation-induced lung fibrosis.

INTRODUCTION

The lung is the major dose-limiting organ in the treatment of cancer in the thoracic region using radiotherapy. The incidence of lung fibrosis depends on several clinical factors, including total dose, dose per fraction, and the combination of radiation and chemotherapy[1–4]. Although clinical observation can often reveal individual differences in the severity of lung fibrosis after radiation therapy, the actual influence of inherent individual factors is difficult to determine in a clinical setting. Geara *et al*. examined the magnitude of individual variation in the incidence and severity of lung fibrosis in a well-defined patient population that underwent concurrent chemoradiation for the treatment of limited small-cell lung carcinomas[5]. They reported that the risk and severity of lung fibrosis analyzed on CT radiographic images increases with total dose and under an accelerated radiation schedule among patients treated with chemoradiation, although patient-to-patient heterogeneity was evident, suggesting that the risk of lung fibrosis is strongly affected by inherent factors that vary among individuals. Roach *et al*. analyzed the incidence of radiation pneumonitis in 1,911 patients treated for lung cancer[6]. They found that large total doses and large doses per fraction are the main independent determinants of radiation pneumonitis. However, they also noted that the data did not perfectly fit their model, suggesting an inherent variation in the individual risk of developing radiation pneumonitis. The clinical observations on inherent variation in lung radiosensitivity correlate closely with experimental data obtained from laboratory animals. Investigations into the mechanism of radiation-induced lung damage through the use of animal models should have a powerful influence on the molecular studies of individual radiosensitivity[7,8]. We previously defined the variation in radiosensitivity of the skin among A/J, C3H/HeMs, C57BL/6J, C.B.17/Icr-scid, and C3H-scid mice[9]. The variation between murine strains in macroscopic and histopathologi-

*Corresponding author: Phone: +81-43-206-3062,
Fax: +81-43-206-3062,
E-mail: mayumii@nirs.go.jp
RadGenomics Project, Frontier Research Center, National Institute of Radiological Sciences. Anagawa 4, 9, 1, Inage-ku, Chiba-shi, 263-8555, Japan.

cal changes in skin during the progression and resolution of damage caused by irradiation suggests an interstrain variation in the expression of genes involved in injury, apoptosis, repair, and remodeling. Several other investigators have also reported the risk of developing lung fibrosis after lung irradiation among murine stains, and others have found transcriptional differences among strains after ionizing irradiation[8,10–19]. Johnston investigated the chronic expression of specific chemokine and chemokine receptors during the fibrotic phase induced by thoracic irradiation as well as the expression of TGF-beta and transcriptomes in an attempt to identify genes involved in lung inflammation after irradiation[20,21]. Recently, the important role of certain molecules, such as CD44 and hyaluronan (HA), during the repair of inflammation in lung fibrosis has been identified[22–28]. CD44 is a transmembrane adhesion receptor and the major cell-surface receptor for the nonsulfated glycosaminoglycan hyaluronan. CD44 plays an important role in the clearance of HA and mediates cell-matrix interactions involved in lymphocyte extravasation.

Here we investigated the appearance of CD44 and HA in the lungs of inbred C57BL/6J and C3H/HeMs mice to reveal the interstrain difference during inflammation caused by irradiation. We also examined the expression analysis of several genes to gain insights into the interstrain differences in radiosensitivity.

MATERIALS AND METHODS

Mice

Twelve-week-old female inbred C57BL/6J and C3H/HeMs mice were bred and maintained in the specific-pathogen-free mouse colony of the National Institute of Radiological Sciences. A maximum of five mice were housed in each cage. A total of 400 mice were used for pathological and transcriptional experiments. The study protocol was reviewed and approved by the NIRS Institutional Animal Care and Use Committee (protocol number 13–1073).

Irradiation

After anesthesia with pentobarbital (50 mg/kg body weight), the mice were immobilized with tape on Lucite plates, and the thorax was locally irradiated with 137-Cs gamma rays at an FSD of 21 cm with an average exposure rate of 1.4 Gy/min. A doughnut-shaped radiation field with a 30 mm rim collimated the vertical beam for several mice at each session. The two doses of radiation, i.e., 10 Gy and 20 Gy, were used, except for transcriptome assay. A single dose of 10 Gy was applied to transcriptome assay. The controls received no irradiation.

Tissue isolation

The animals were sacrificed and immediately dissected for lung extraction at 1, 12, and 72 hours after irradiation or without irradiation (non-exposed control) for histological investigation and transcriptome assays, and they were sacrificed at times corresponding to the latent period (1, 12, and 72 hours postirradiation), the pneumonic phase (2, 4, 8, and 16 weeks postirradiation), and the start of the fibrotic phase (24 weeks postirradiation) for histological investigation. The lungs without irradiation were extracted at each time as mentioned above as control. Whole lungs were immediately removed after sacrifice with a perfusion of 10% neutralized formalin for pathological analysis. For expression analysis, the lung lobes were chopped and placed in RNAlater (Ambion, Austin, TX, USA) to isolate RNA. Samples in RNAlater were stored at –20°C.

Histopathology

One lobe from the left lung of each mouse was fixed in 10% neutralized formalin, paraffin-embedded, and sectioned at an average thickness of 3 micrometers. The sections were routinely stained with hematoxylin and eosin (H&E), and collagen fibers were detected using Masson's trichrome stain. The surface of measurements for three fields was total, and the arithmetic mean was calculated. The collagen fiber areas are expressed as the average per field.

Immunohistochemistry

Macrophages were detected by the use of anti-F4/80 antibody (Biomedicals AG, Switzerland). CD44 was detected with mouse anti rat CD44 monoclonal antibody (BIOCAR-

Table 1. Primers.

Name	Primers	
Cap1	F	tttaacgagttcccagtcccc
	R	gcacaggacccatgtatttgc
Il18	F	aagatgattagcacacatgcgc
	R	tctataaatcatgcagcctcgg
Rad51ap1	F	tcaaagcctttctgtccttcg
	R	tgtgattacagacgtgccgc
Mmp12	F	tcaattggaatatgacccccctg
	R	cagcaagcacccttcactacatt
Per3	F	gctgtaaagatgtcacaccccc
	R	tcaatgactggcgtttcagagt
Ltf	F	tgctaaccagaccagatcctgc
	R	cttgttctcacccttctcatcacc
Ifi202a	F	tccacctcttctgctttcacct
	R	tgaccttgacgaaactgtggtct
Gapd	F	ccagaacatcatccctgcatc
	R	atgcctgcttcaccaccttc

TA, CA, USA), and HA was detected by the use of hyaluronic acid binding protein (HABP) (Seikagaku Corp., Tokyo, Japan). Sections were incubated for 1.5 hours at 37°C with mouse antirat CD44 monoclonal antibody (diluted 1:500 in PBS) and with hyaluronic acid-binding protein (HABP antibody diluted 1:300). All tissue sections were deparaffinized and rehydrated in graded alcohols. Before anti-F4/80 staining, nonspecific protein binding was blocked for 20 min with 1.5% horse or rabbit serum, respectively. Antigen-antibody complexes were detected by the use of the Vectastain mouse ABC peroxidase kit (Vector Laboratories, Burlingame, CA, USA), according to the manufacturer's instructions. Inherent peroxidase activation was blocked for 3 min with 1% H_2O_2. Sections were incubated for 1.5 hours with biotinylated secondary antibody, followed by 45 min with ABC reagent. Bound peroxidase was then detected after a 5-min reaction with diaminobenzidine.

Scoring positive cells and of lesions

To ensure objectivity, we standardized and consistently applied a blind evaluation with respect to stain throughout the study. We initially examined whole lung sections and estimated the extent of altered lung parenchyma, then selected and analyzed lung sections of nonoverlapping fields (× 40 objective). The sum of measurements from the three fields was totaled and the arithmetic mean calculated. Positive cell counts are expressed as the average number of cells per field. To assess the lesions with positive HA, we score the extent of positive area with HA staining per field (× 40 objective) by use of the arbitrary scale. The scoring system consisted of 4 degrees, ranging score 0.5 to 3 as follows: score 0.5; less than 10%, score 1.0; 10% to 33%, score 2.0; 34% to 66%, score 3.0; more than 67%.

Computer-aided morphometric analysis

To evaluate fibrosis, sections were stained with Masson's trichrome to detect collagen fibers. Fibrotic areas identified by blue staining were measured with a color image analyzer (Win ROOF, Mitani Inc., Tokyo, Japan) in 3 areas (0.15~ 0.4 mm^2 each) of the lung, and the average area was estimated.

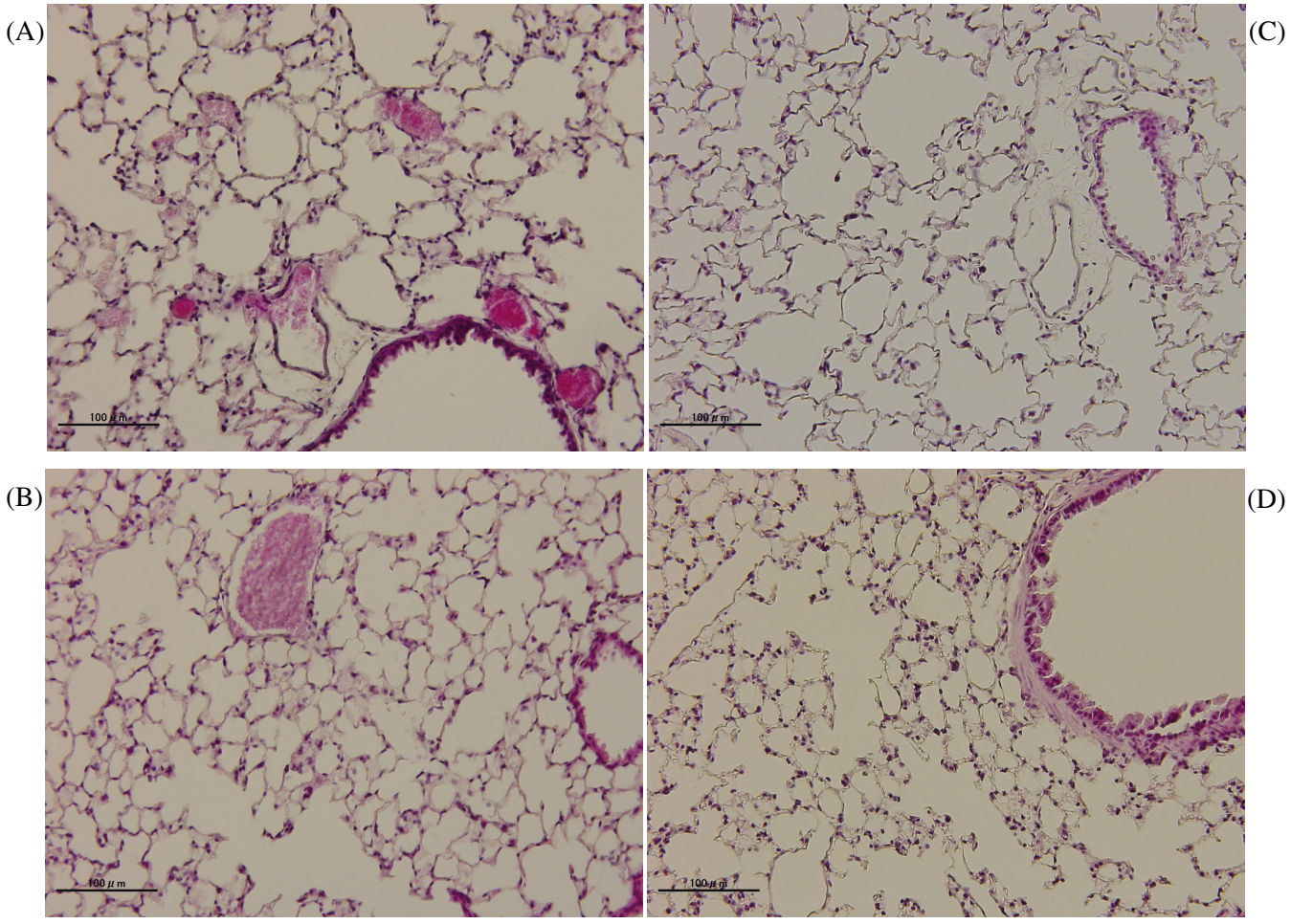

Fig. 1. Inflammatory foci that appeared at 72 hours after at 20Gy; (A) C3H/HeMs, (B) C57BL/6J. Non- exposed control; (C) C3H/HeMs, (D) C57BL/6J.

Microarray analysis

Total RNA was extracted from non-exposed lungs as control, and lungs dissected at 1, 12, and 72 h after irradiation. Agilent's Mouse cDNA Microarray Kit (Agilent Technologies, Palo Alto, CA) features more than 8,500 Incyte mouse UniGene 1 clones per microarray. This kit and the Agilent Direct-Label cDNA Synthesis Kit (Agilent Technologies, Palo Alto, CA) were used throughout the study. Total RNA (7 micrograms) from 3 mice per group was pooled, and Cy5-dCTP or Cy3-dCTP (Perkin-Elmer, Boston, MA) labeled cDNA was synthesized from 20 microgram of the pooled RNA. Reference cDNA, which was labeled identically for each array slide, was synthesized from commercially available RNA from 10 organs (FirstChoiceTM Total RNA; Ambion, Austin, TX). Labeled cDNA was purified with CyScribe GFX Purification Kits (Amersham Biosciences, Piscataway, NJ). Fluorescent array images were collected for Cy3 and Cy5 emissions with an Agilent dual-laser Microarray Scanner (Agilent Technologies, Palo Alto, CA, USA). Image intensity data were extracted with Feature Extraction software (Agilent Technologies, Palo Alto, CA, USA) and normalized by Rank Consistency Filter of Feature Extraction software. The data were further processed by means of the Rosetta Resolver Data Analysis System (Rosetta Biosoftware, Kirkland, WA). Differentially expressed genes were selected by the use of an up- or down-regulation value of more than twofold.

Quantitative RT-PCR

First strand cDNA was synthesized from total RNA (2 micrograms) by the use of reverse transcriptase and of oligo d(T)12-18 primer. All primer sequences were shown in Table 1. Pooled cDNA samples from each group were diluted × 5 in TE buffer. Amplification reactions proceeded by the use of iQ SYBR Green Supermix (Bio-Rad, Hercules, CA). The primer3 program (http://www-genome.wi.mit.edu/genome_software/other/primer3.html) determined primer sets for each gene. For all primers, the specificity of amplifications was checked by agarose gel electrophoresis. These ampli-

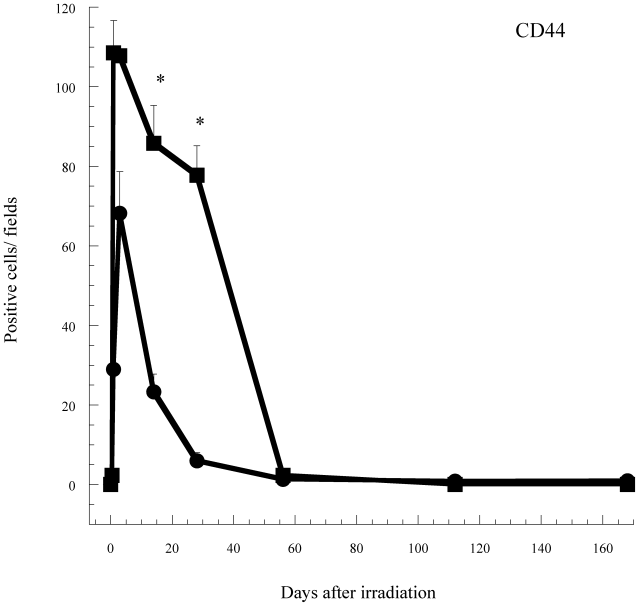

Fig. 3. Accumulation of CD44 over time after irradiation. Murine thoracic regions were irradiated with one dose of 10 Gy. *: $p < 0.005$. C3H/HeMs (solid square), C57BL/6J (solid circle).

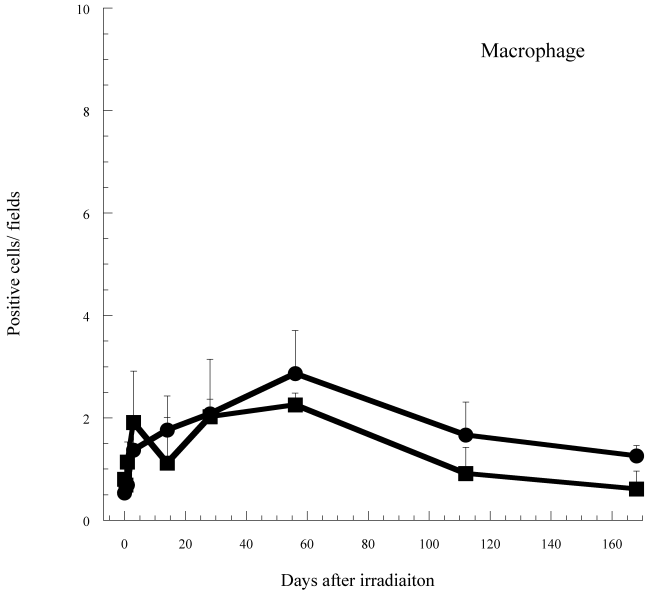

Fig. 2. Number of macrophages that appeared with time after irradiation. Murine thoracic regions were irradiated with one dose of 10 Gy. C3H/HeMs (solid square), C57BL/6J (solid circle).

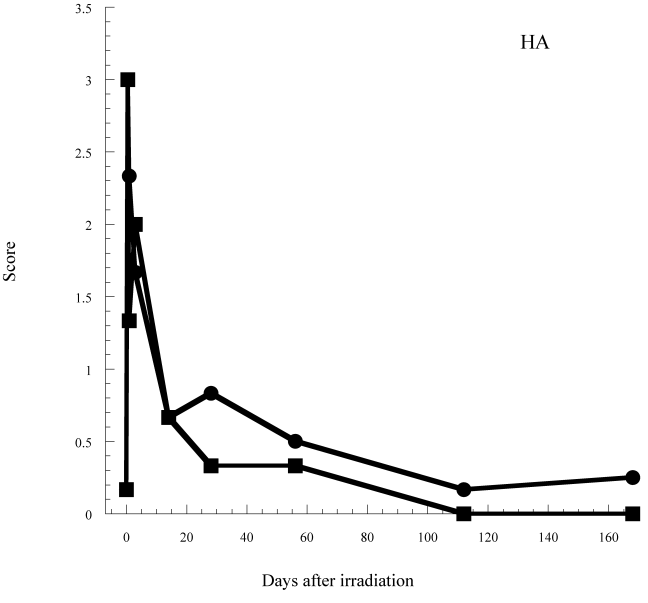

Fig. 4. Score of HA over time after irradiation. Murine thoracic regions were irradiated with one dose of 10 Gy. C3H/HeMs (solid square), C57BL/6J (solid circle).

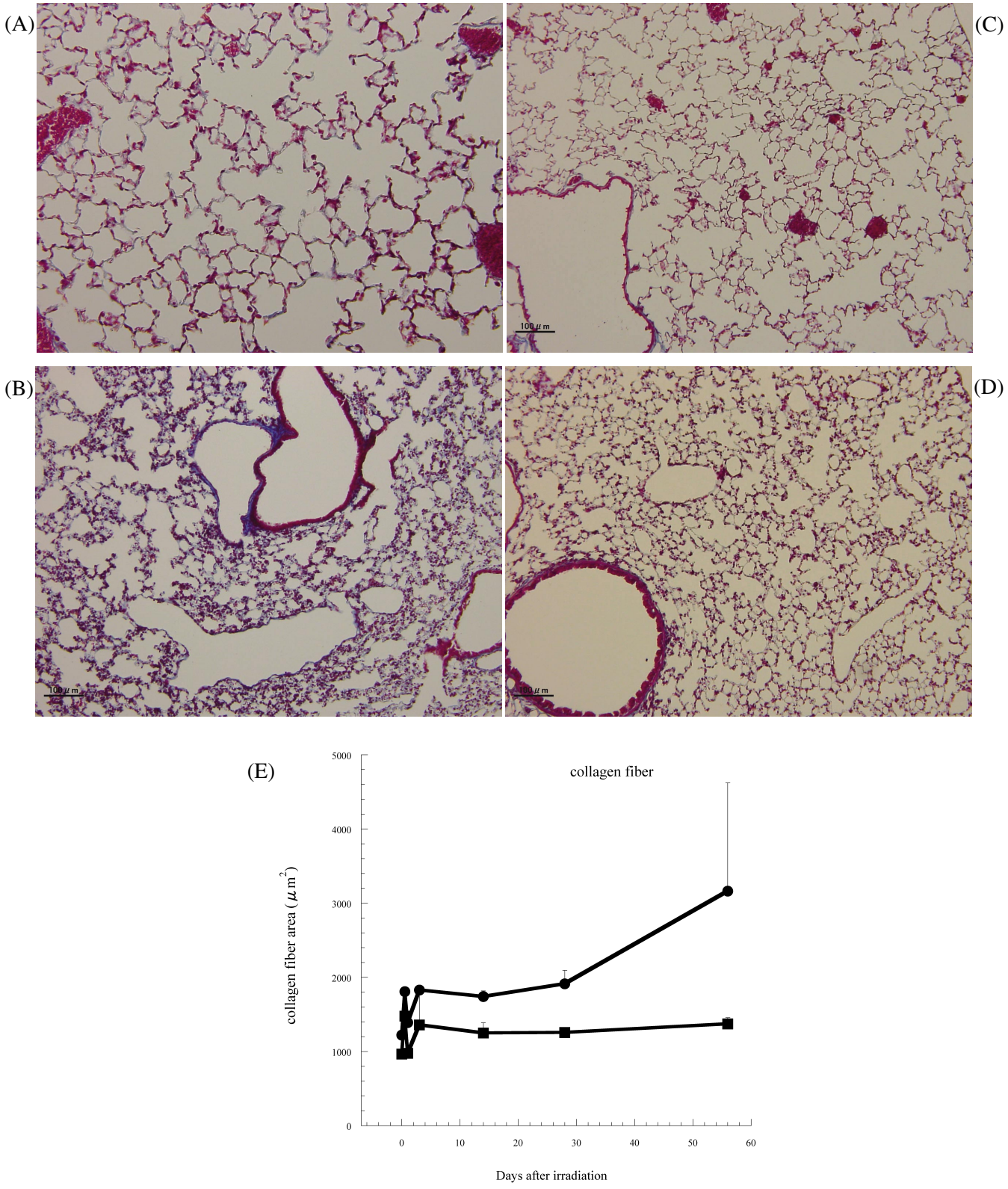

Fig. 5. Accumulation of collagen fibers over time after irradiation. Murine thoracic regions were irradiated with one dose of 20 Gy; (A) C3H/HeMs, (B) C57BL/6J. Non- exposed control; (C) C3H/HeMs, (D) C57BL/6J. (E) C3H/HeMs (solid square), C57BL/6J (solid circle).

cons were extracted and purified from gels. We determined the amount of purified amplicons by measuring the 260 nanometer absorbance. These were subsequently applied as standards for quantitative PCR. The primer concentration was 500 nM in a final volume of 15 microliters, which contained 5 microliters of cDNA sample. Quadruplicate reactions proceeded by use of the iCycler system (Bio-Rad, Hercules, CA). Thermal cycling conditions were as follows: 10 min at 95°C, followed by 37 cycles at 95°C, 57°C, and 72°C for 30 seconds each. All PCR products were verified by melting point analysis. Gene expression was quantified with reference to a calibration curve drawn from serial dilutions of measured target fragment. We determined the threshold level of fluorescence and eliminated interexperimental errors by using subcloned mouse Gapd cDNA and Gapd specific primers in each experiment as additional standards. Complementary DNA was synthesized twicefrom the same RNA samples, and all assays were performed in duplicate. The relative mRNA levels of the indicated genes were measured with quantitative PCR assay. Data from the RT-PCR analysis were normalized to mRNA concentrations, compared to the known amounts of cDNA fragments of glyceraldehyde-3-phosphate dehydrogenase (Gapd), and were shown by bar graph relative to the mRNA level of non-exposed C57BL/6J mice.

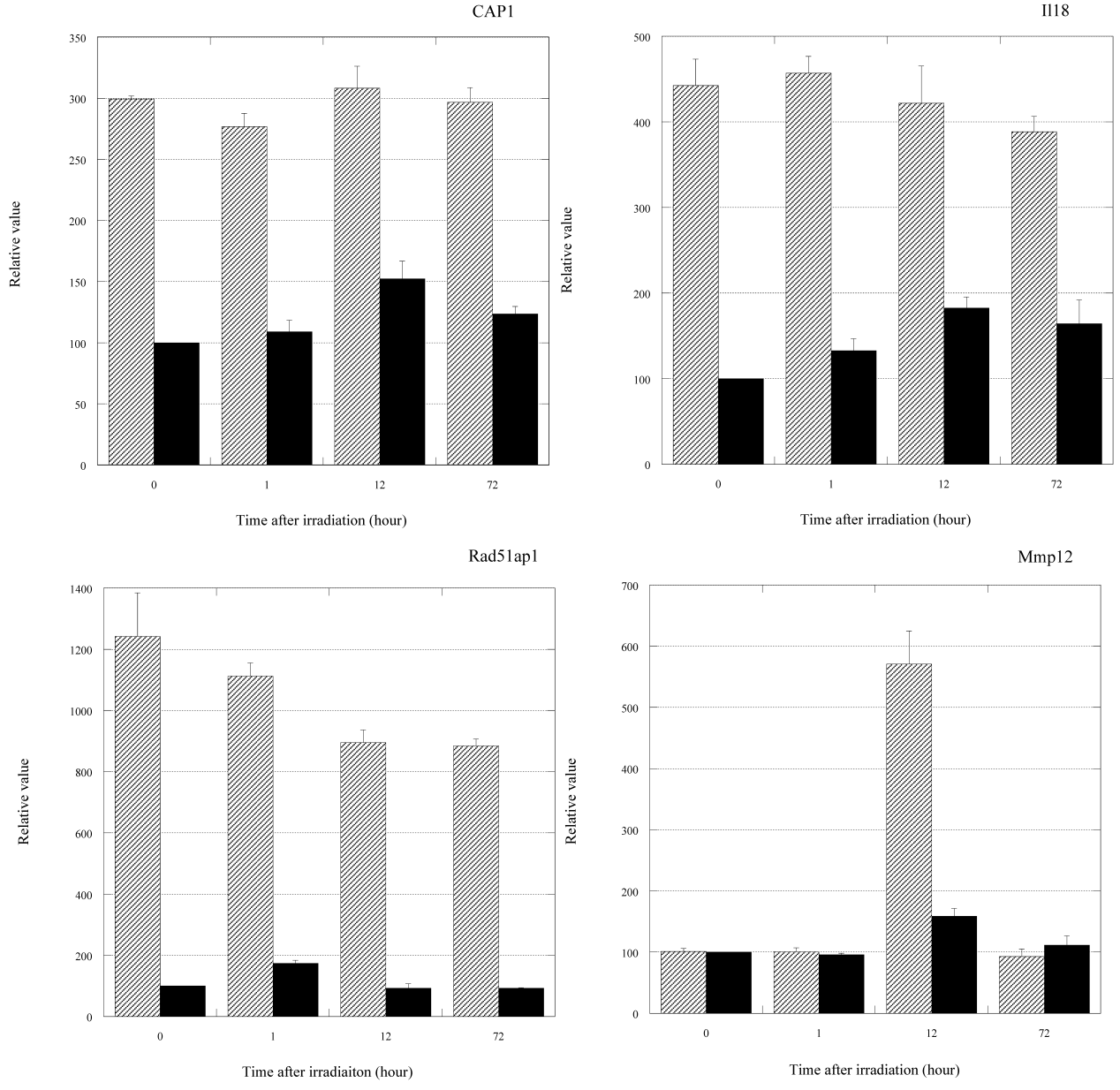

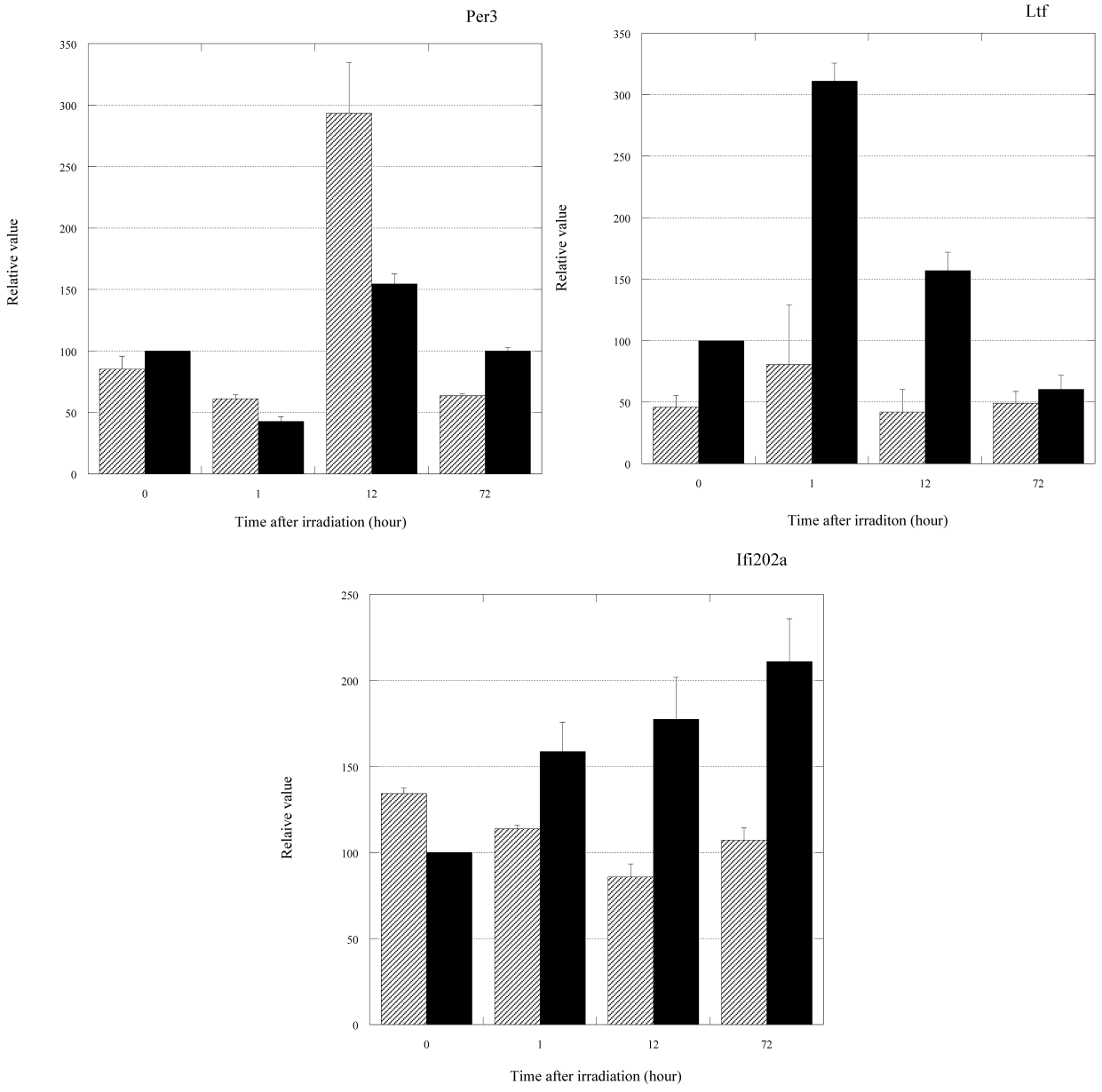

Fig. 6. Gene expression over time after irradiation. Murine thoracic regions were irradiated with one dose of 10 Gy. The relative mRNA levels of the indicated genes (A: CAP1, B: Il18, C: Rad 51ap1, D: Mmp12, E: Per3, F: Ltf, G: Ifi202a) were measured with quantitative PCR assay. Data from the RT-PCR analysis were normalized to mRNA concentrations compared to the known amounts of cDNA fragments of glyceraldehyde-3-phosphate dehydrogenase (Gapd) and were shown by bar graph relative to the mRNA level of non-exposed C57BL/6J mice. C3H/HeMs (shaded column), C57BL/6J (solid column).

Statistical analysis

The differences in numbers of positive cells with CD44, or the areas of collagen fibers between C57BL/6J and C3H/HeMs mice, were tested by parametorical Student's t-test.

RESULTS

Histology

The histological alterations in irradiated lungs conformed to those described, including macrophage infiltration and desquamation of epithelial cells from the alveolar walls. Interstitial fibrosis was evident within lesions consisting of aggregations of macrophages, or lymphocytes. Small areas of fibrosis initially appeared in C57BL/6J mice at 4 weeks postirradiation with 20 Gy, whereas small inflammatory lesions appeared at 4 and 8 weeks after 20 and 10 Gy, respectively. The numbers of foci of inflammation appeared to decline slightly between 8 and 12 weeks when the first

fibrotic foci appeared. The severity of these histological changes was strain-dependent. The alveoli septa were thickened by an infiltration of inflammatory cells, and alveoli were obliterated in lungs from C57BL/6J mice. Inflammatory foci obviously preceded the development of fibrosis. More fibrosis foci developed during the late phase in C57BL/6J mice than in C3H/HeMs mice. On the other hand, C3H/HeMs mice did not develop fibrotic scars, but more late deaths occurred.

Immunohistochemistry

Inflammatory foci initially appeared at 72 h to 4 weeks after at 20 Gy (Fig. 1). Obvious inflammatory foci were not observed in mice irradiated at 10 Gy. These foci remained as areas of mild cellular infiltration and macrophages clustered in small groups within alveoli. Lymphocytes, macrophages, and neutrophils in the radiation-induced fibrosis area suggest their involvement in the fibrotic response. The numbers of macrophages in inflammatory foci did not apparently change with postirradiation time or did not differ between the two strains at 10 Gy (Fig. 2). At 24 h and from 2 to 4 weeks postirradiation, fourfold more CD44 positive cells had accumulated in the lungs of C3H/HeMs than in the lungs of C57BL/6J mice at 10 Gy (Fig. 3). At sites of lung inflammation, HA accumulated at 12 h after irradiation, and the rapid resolution was achieved within 2 weeks in the lungs in both C57BL/6J mice and C3H/HeMs mice at 10 Gy (Fig. 4). Connective tissue elements increased at the expense of parenchymal elements in the lungs after 20 Gy of irradiation. A histological investigation of C57BL/6J mice lungs revealed dense collagen accumulation at 8 weeks (Fig. 5A, 5B).

Gene expression analysis

We used cDNA microarrays as screening various genes that were up- or down-regulated after irradiation with strain differences. Non-exposed mice and the irradiated mice at 12, 24, and 72 h after irradiation were sacrificed. Their lungs were extracted for expression analysis. The clustering and display programs of Rosetta Resolver Data Analysis System were used for analysis. Through the basal RNA expression of genes in non-exposed lung and the regulated expression ratio induced by irradiation, some 600 genes were significantly regulated across the groups of samples, that is, at least a twofold difference. A supervised hierarchical clustering algorithm allowed us to cluster the lung tissues on the basis of their similarities measured over these 600 genes. The groups equaling the strains were the dominant feature in the two-dimensional display, suggesting that the expression pattern can be divided into the types on the basis of strain difference. To gain insight into the genes of the dominant expression signature, the number of genes in the strain classifier was optimized by expression pattern. Seventy-three genes were selected. The functional annotation for these genes provides insight into the underlying biological mechanism. We selected several genes, mainly those related with the host defense mechanism leading to the pathological change of lungs after irradiation, including genes such as Ltf, Ifi202a, Il18, Mmp12, Rad51ap1, Per3, and Cap1, for RT-PCR assay. The expression of Cap1 and Il18 was constantly higher for 72 h after irradiation in C3H/HeMs mice than in C57BL/6J mice. The expression of Rad51ap1 was constantly higher in C3H/HeMs mice for 72 h after irradiation and at non-exposed status than in C57BL/6J mice. Mmp12 and Per3 was more induced at 12 h after irradiation in C3H/HeMs mice than in C57BL/6J mice. The expression of Ltf was higher at 1 h after irradiation, and that of Ifi202a was more induced at 72 h in C57BL/6J mice than in C3H/HeMs mice. (Fig. 6)

DISCUSSION

Even with recent advances in technology, a study of patient factors contributing to the normal tissue response still has important implications for radiotherapy. The ultimate aim of our research is to clarify the mechanisms of heterogeneity in response to ionizing radiation arising from individual genetic variations among humans. The present study was designed to elucidate the mechanisms through which ionizing radiation causes the interstrain differences during the induction of a fibrotic response in pulmonary parenchyma.

Lung injury after radiation is often accompanied by an inflammatory response, which might result in the activation and expansion of the resident macrophage population through the recruitment of new cells. These activated macrophages are the source of many growth factors and as such play a key role in wound healing. In this study, inflammatory foci appeared 4 weeks after irradiation, and numbers of macrophages identically and time-dependently fluctuated in both strains of irradiated mice. Instead, the numbers of CD44-positive cells varied among strains. It is known that macrophages predominate in the earliest fibrotic lesions, and the frequency of macrophages decreases during the latent period and the early phase[18]. Lorimore[29] demonstrated a complexity of macrophage activation following radiation that is genotype dependent, indicating that the *in vivo* macrophage responses to radiation damage are genetically modified processes. When they quantified macrophage numbers either immunohistochemically by using antibody against F4/80, or morphologically by using electron microscopy, the two strains, such as C57BL/6 and CBA/Ca, which showed different radiosensitivity, contained similar numbers of macrophages. When they are considered with our data, it is suggested that the different radiosensitivity through macrophages is not simply due to the presence of different numbers of macrophages, but must instead be due to different levels of enzyme activity per cell.

The pathogenesis of pulmonary fibrosis typically exhibits overlapping phases of this inflammation response and matrix deposition. Appropriate repair after tissue injury and inflammation requires a resolution of the inflammatory response and the removal of extracellular matrix breakdown products. In this study, we investigated CD44 positive cells in the pulmonary parenchyma and found an increase in the number of CD44 positive cells, especially in radioresistant mice, which would play a critical role in HA homeostasis following lung injury[26]. At sites of inflammation and tissue injury, low molecular weight HA species accumulate and have proinflammatory functions. Under physiological conditions, HA equilibrium in the lung is maintained by local removal in the alveolar interstitium, primarily by alveolar macrophages. Therefore CD44 plays a critical role in HA homeostasis following lung injury, and this influences the recovery from pulmonary inflammation. We found more CD44 positive cells in C3H/HeMs mice suggesting that matrix deposit clearance is more efficient than in C57BL/6J mice. However, HA content was not different within 2 weeks between the lungs of C57BL/6J mice and C3H/HeMs mice. We need further research for the qualification of HA species and at a different timing.

Sharplin and Franko have published many papers on strain-dependent differences in the effects of irradiation by a quantitative histological study[8,13,15]. They used hematoxylin and eosin staining and phosphotungustic acid hematoxilin staining to detect fibrillar material in the alveoli, and we detected collagen fibers, using Masson's trichrome stain, and measured the amount of collagen fibers with a color image analyzer. We observed that C57BL/6J mice lungs revealed dense collagen accumulation at 8 weeks, and this result is in agreement with their tremendous work. Many reports have also noted that TGF-beta is a key causative agent of lung fibrosis[19,20]. The predominant localization of TGF-beta in the lung from C57BL/6J mice, which was also detected in the present study, supported the notion that this cytokine is involved in the pathogenesis of more severe pneumonitis (data not shown).

Furthermore, expression analysis was performed to identify genes involved in lung inflammation after irradiation in animal models to shed some light on the mechanism of strain-dependent lung damage. The possible mechanisms include the immunological response, inflammatory reactions, alveolar epithelial injury, increased sequestration of inflammatory cells in the microvasculature, increased expression of pro-inflammatory mediators, fibrotic change, and the accumulation of collagen fibers. It is noteworthy that the first classification by unsupervised clustering derived the samples into two large groups: C3H/HeMs mice and C57BL/6J mice instead of postirradiation time. After this screening procedure, we selected several candidate genes related with the inflammatory or immunological response for RT-PCR assays.

Higher expression levels of Cap1, Il18, and Rad51ap1 were observed in lungs of non-exposed control and irradiated lungs of C3H/HeMs mice than in lungs of C57BL/6J mice. Higher expression levels of Mmp12 and Per3 at 12 h after irradiation were also observed. In histology, a higher level of CD44 positive cells was observed for 8 weeks after irradiation in the lungs of C3H/HeMs mice than in C57BL/6J mice, and C3H/HeMs mice finally presented less damaged lungs in the pneumonic phase and the fibrotic phase after irradiation than C57BL/6J mice did.

CAP1 was identified by Vojtek *et al.*[30]. They found ectopically expressed mouse CAP protein in migrating cells at the leading edge. IL-18 is a member of the IL-1 cytokine family, and an important mediator of peripheral inflammation as well as the host defense response[31]. Mmp12 is an MMP[32] and accounts for most macrophage-derived elastase activity, and the migration of macrophages is accompanied by Mmp12-dependent tunnel formation and by neovascularization[33]. It might be important to mention the change of Rad51ap1, which is not related with inflammation. Rad51ap1, alternate RAB22, is a novel gene product that interacts with Rad51 *in vitro* and *in vivo*[34]. RAD51 is known to be involved in the homologous recombination and repair of DNA. This protein is also known to interact with BRCA1 and BRCA2. For appropriate repair after irradiation, it might be important to have a balance between the inflammatory response and the removal of extracellular matrix breakdown products.

Per3 is one of eight core circadian genes[35]. Circadian genes are also known to respond directly to genotoxic stress, since sleep disorder is common among patients receiving radiation treatment. Our findings that Per3 might have an important role for radiosensitivity would be a new discovery of this gene function.

The expression levels of Ltf and Ifi202a were higher after irradiation in C57BL/6J mice than in C3H/HeMs mice in this study. The iron-binding glycoprotein, Ltf, is an important integral part of the cytokine-induced cascade during insult-induced metabolic imbalance, and several cell surface receptors are implicated in the unique properties of Ltf, including those on macrophages and lymphocytes[36,37]. Ltf can also control the physiological balance between reactive oxygen species (ROS) production and the rate of their elimination, which naturally protects against oxidative cell injury[38,39]. A high expression of Ltf might indicate the activated cytokine-induced cascade or ROS production after irradiation in C57BL/6J mice. Ifi202 gene is part of the interferon-activatable murine gene 200 cluster on chromosome 1q21-q23[40], which is involved in the control of cell proliferation, differentiation, and apoptosis[34,41,42].

This study demonstrated that several gene expressions of lung between two strains might be correlated with differences of morphological alterations in lung, providing insight into the fundamental pathways that are responsible for the

initiation and progression of adverse effects.

We could not conclude which genes could be a most useful biomarker of radiosensitivity among strains, and we realized that strain-dependent radiosensitivity is caused by the coordination of many factors. Further investigation with bioinformatics and more experiments to identify the key genes is underway in our laboratory. Rubin *et al*. reported that genetic variation influences the development of bleomycin-induced pulmonary fibrosis, showing that major histocompatibility complex (H-2) genes modulate the intensity of disease[14]. Schrier suggested that major histocompatibility complex (H-2) genes modulate the intensity of disease, whereas the non-H-2 haplotype responds with different intensities, suggesting that non-H-2 genes play a permissive role in the development of the disease[43]. These studies, including ours, are germane to investigations into the mechanisms of pneumonitis or pulmonary fibrosis after irradiation to understand genetic predisposition to the development of pulmonary damage.

CONCLUSION

The present study examined the histology and gene expression in the lungs of inbred C57BL/6J and C3H/HeMs mice after irradiation to gain insight into molecular and physiological variance for strain-dependent lung fibrosis. The predominant accumulation of collagen fibers in the lungs of C57BL/6J mice suggested its involvement in the pathogenesis of lung fibrosis. In C3H/HeMs mice, a more rapid clearance of matrix deposit after inflammation was observed than in C57BL/6J. The expression analysis showed that the mouse Ltf, Ifi202a, Il18, Per3, Mmp12, Cap1, and Rad51ap1 genes are potentially involved in interstrain differences in the pathogenesis of radiation-induced lung damage.

ACKNOWLEDGMENTS

We wish to express our deep thanks to Mr. Tatsuo Hayao and Mrs. Yuriko Ogawa for their animal care services. Mrs. Etsuko Hagiwara is gratefully acknowledged for her graphical assistance.

REFERENCES

1. McDonald, S., Rubin, P., Maasilta, P. (1989) Response of normal lung to irradiation. Tolerance doses/tolerance volumes in pulmonary radiation syndromes. Front. Radiat. Ther. Oncol. **23**: 255–276, 299–301.
2. Lingos, T. I., Recht, A., Vicini, F., Abner, A., Silver, B., Harris, J. R. (1991) Radiation pneumonitis in breast cancer patients treated with conservative surgery and radiation therapy. Int. J. Radiat. Oncol. Biol. Phys. **21**: 355–360.
3. Mah, K., Keane, T. J., Van, Dyk. J., Braban, L. E., Poon, P. Y., Hao, Y. (1994) Quantitative effect of combined chemotherapy and fractionated radiotherapy on the incidence of radiation-induced lung damage: a prospective clinical study. Int. J. Radiat. Oncol. Biol. Phys. **28**: 563–574.
4. McDonald, S., Rubin, P., Phillips, T. L., Marks, L. B. (1995) Injury to the lung from cancer therapy: clinical syndromes, measurable endpoints, and potential scoring systems. Int. J. Radiat. Oncol. Biol. Phys. **31**: 1187–1203.
5. Geara, F.B., Komaki, R., Tucker, S. L., Travis, E. L., Cox, J. D.(1998) Factors influencing the development of lung fibrosis after chemoradiation for small cell carcinoma of the lung: evidence for inherent interindividual variation. Int. J. Radiat. Oncol. Biol. Phys. **41**: 279–286.
6. Roach, M. 3rd., Gandara, D. R., You, H. S., Swift, P. S., Kroll, S., Shrieve, D. C., Wara, W. M., Margolis, L., Phillips, T. L. (1995) Radiation pneumonitis following combined modality therapy for lung cancer: analysis of prognostic factors. J. Clin. Oncol. **13**: 2606–2612.
7. Fedorocko, P., Egyed, A., Vacek, A. (2002) Irradiation induces increased production of haemopoietic and proinflammatory cytokines in the mouse lung. Int. J. Radiat. Biol. **78**: 305–313.
8. Sharplin, J., Franko, A. J. (1989) A quantitative histological study of strain-dependent differences in the effects of irradiation on mouse lung during the intermediate and late phases. Radiat. Res. **119**: 15–31.
9. Iwakawa, M., Noda, S., Ohta, T., Ohira, C., Lee, R., Goto, M., Wakabayashi, M., Matsui, Y., Harada, Y., Imai, T. (2003) Different radiation susceptibility among five strains of mice detected by a skin reaction. J. Radiat. Res. **44**: 7–13.
10. Down, J. D., Steel, G. G. (1983) The expression of early and late damage after thoracic irradiation: a comparison between CBA and C57B1 mice. Radiat. Res. **96**: 603–610.
11. Down, J. D. (1986) The nature and relevance of late lung pathology following localised irradiation of the thorax in mice and rats. Br. J. Cancer Suppl. **53**: 330–332.
12. Down, J. D., Nicholas, D., Steel, G. G.(1986) Lung damage after hemithoracic irradiation: dependence on mouse strain. Radiother. Oncol. **6**: 43–50.
13. Sharplin, J., Franko, A. J. (1986) Pulmonary oedema during the latent period after irradiation of murine lung. Br. J. Cancer. Suppl. **7**: 336–339.
14. Rubin, P., Finkelstein, J. N., Siemann, D. W., Shapiro, D. L., Van, Houtte, P., Penney, D. P. (1986) Predictive biochemical assays for late radiation effects. Int. J. Radiat. Oncol. Biol. Phys. **12**: 469–476.
15. Sharplin, J., Franko, A. J. (1989) A quantitative histological study of strain-dependent differences in the effects of irradiation on mouse lung during the early phase. Radiat. Res. **119**: 1–14.
16. Franko, A. J., Sharplin, J., Ward, W. F., Hinz, J. M. (1991) The genetic basis of strain-dependent differences in the early phase of radiation injury in mouse lung. Radiat. Res. **126**: 349–356.
17. Finkelstein, J. N., Johnston, C. J., Baggs, R., Rubin, P. (1994) Early alterations in extracellular matrix and transforming growth factor beta gene expression in mouse lung indicative of late radiation fibrosis. Int. J. Radiat. Oncol. Biol. Phys. **28**: 621–631.

18. Franko, A. J., Sharplin, J. (1994) Development of fibrosis after lung irradiation in relation to inflammation and lung function in a mouse strain prone to fibrosis. Radiat. Res. **140**: 347–355.
19. Rube, C. E., Uthe, D., Schmid, K. W., Richter, K.D., Wessel, J., Schuck, A., Willich, N., Rube, C. (2000) Dose-dependent induction of transforming growth factor beta (TGF-beta) in the lung tissue of fibrosis-prone mice after thoracic irradiation. Int. J. Radiat. Oncol. Biol. Phys. **47**: 1033–1042.
20. Johnston, C. J., Piedboeuf, B., Baggs, R., Rubin, P., Finkelstein, J. N. (1994) Differences in correlation of mRNA gene expression in mice sensitive and resistant to radiation-induced pulmonary fibrosis. Radiat. Res. **142**:197–203.
21. Johnston, C. J., Williams, J. P., Okunieff, P., Finkelstein, J. N. (2002) Radiation-induced pulmonary fibrosis: examination of chemokine and chemokine receptor families. Radiat. Res. **157**: 256–265.
22. Bartolazzi, A., Peach, R., Aruffo, A., Stamenkovic, I. (1994) Interaction between CD44 and hyaluronate is directly implicated in the regulation of tumor development. J. Exp. Med. **180**: 53–66.
23. Yu, Q., Toole, B. P., Stamenkovic, I. (1997) Induction of apoptosis of metastatic mammary carcinoma cells *in vivo* by disruption of tumor cell surface CD44 function. J. Exp. Med. **186**: 1985–1996.
24. DeGrendele, H. C., Estess, P., Siegelman, M. H. (1997) Requirement for CD44 in activated T cell extravasation into an inflammatory site. Science. **278**: 672–675.
25. Wang, Q., Teder, P., Judd, N. P., Noble, P. W., Doerschuk, C. M. (2002) CD44 deficiency leads to enhanced neutrophil migration and lung injury in Escherichia coli pneumonia in mice. Am. J. Pathol. **161**: 2219–2228.
26. Teder, P., Vandivier, R. W., Jiang, D., Liang, J., Cohn, L., Pure, E., Henson, P. M., Noble, P. W. (2002) Resolution of lung inflammation by CD44. Science. **296**: 155–158.
27. Laurent, T. C., Fraser, J. R. (1992) Hyaluronan. FASEB. J. **6**: 2397–2404.
28. Savani, R. C., Hou, G., Liu, P., Wang, C., Simons, E., Grimm, P. C., Stern, R., Greenberg, A. H., DeLisser, H. M., Khalil, N. (2000) A role for hyaluronan in macrophage accumulation and collagen deposition after bleomycin-induced lung injury. Am. J. Respir. Cell. Mol. Biol. **23**: 475–484.
29. Lorimore, S. A., Coates, P. J., Scobie, G. E., Milne, G., Wright, E. G. (2001) Inflammatory-type responses after exposure to ionizing radiation *in vivo*: a mechanism for radiation-induced bystander effects? Oncogene. **20**: 7085–7095.
30. Moriyama, K., Yahara, I. (2002) Human CAP1 is a key factor in the recycling of cofilin and actin for rapid actin turnover. J. Cell. Sci. **115**: 1591–1601.
31. Hoshino, T., Wiltrout, R. H., Young, H. A. (1999) IL-18 is a potent coinducer of IL-13 in NK and T cells: a new potential role for IL-18 in modulating the immune response. J. Immunol. **162**: 5070–5057.
32. Lanone, S., Zheng, T., Zhu, Z., Liu, W., Lee, C. G., Ma, B., Chen, Q., Homer, R. J., Wang, J., Rabach, L. A., Rabach, M. E., Shipley, J. M., Shapiro, S. D., Senior, R. M., Elias, J. A. (2002) Overlapping and enzyme-specific contributions of matrix metalloproteinases-9 and -12 in IL-13-induced inflammation and remodeling. J. Clin. Invest. **110**: 463–474.
33. Morris, D. G., Huang, X., Kaminski, N., Wang, Y., Shapiro, S. D., Dolganov, G., Glick, A., Sheppard, D. (2003) Loss of integrin alpha(v)beta6-mediated TGF-beta activation causes Mmp12-dependent emphysema. Nature. **422**: 169–173.
34. Mizuta, R., LaSalle, J. M., Cheng, H. L., Shinohara, A., Ogawa, H., Copeland, N., Jenkins, N. A., Lalande, M., Alt, F. W. (1997) RAB22 and RAB163/mouse BRCA2: proteins that specifically interact with the RAD51 protein. Proc. Natl. Acad. Sci. **24**: 6927–6932.
35. Fu, L., Pelicano, H., Liu, J., Huang, P., Lee, C. (2002) The circadian gene Period2 plays an important role in tumor suppression and DNA damage response *in vivo*. Cell. **111**: 41–50.
36. Suzuki, YA., Shin, K., Lonnerdal, B. (2001) Molecular cloning and functional expression of a human intestinal lactoferrin receptor. Biochemistry. **25**: 15771–15779.
37. Ward, P. P, Mendoza-Meneses, M., Cunningham, G. A., Conneely, O. M. (2003) Iron status in mice carrying a targeted disruption of lactoferrin. Mol. Cell. Biol. **23**: 178–185.
38. Tsokos, M., Paulsen, F. (2002) Expression of pulmonary lactoferrin in sudden-onset and slow-onset asthma with fatal outcome. Virchows. Arch. **441**: 494–499.
39. Kruzel, M. L., Zimecki, M. Lactoferrin and immunologic dissonance: clinical implications. (2002) Arch. Immunol. Ther. Exp. (Warsz). **50**: 399–410. Review.
40. Wang, H., Chatterjee, G., Meyer, J. J., Liu, C. J., Manjunath, N. A., Bray-Ward, P., Lengyel, P. (1999) Characteristics of three homologous 202 genes (Ifi202a, Ifi202b, and Ifi202c) from the murine interferon-activatable gene 200 cluster. Genomics. **60**: 281–294.
41. Min, W., Ghosh, S., Lengyel, P. (1996) The interferon-inducible p202 protein as a modulator of transcription: inhibition of NF-kappa B, c-Fos, and c-Jun activities. Mol. Cell. Biol. **16**: 359–368.
42. Wang, H., Ding, B., Liu, C. J., Ma, X. Y., Deschamps, S., Roe, B. A., Lengyel, P. (2002) The increase in levels of interferon-inducible proteins p202a and p202b and RNA-dependent protein kinase (PKR) during myoblast differentiation is due to transactivation by MyoD: their tissue distribution in uninfected mice does not depend on interferons. J. Interferon. Cytokine. Res. **22**: 729–737.
43. Schrier, D. J., Kunkel, R. G., Phan, S. H. (1983) The role of strain variation in murine bleomycin-induced pulmonary fibrosis. Am. Rev. Respir. Dis. **127**: 63–66.

Received on March 11, 2004
1st Revision on June 28, 2004
Accepted on July 1, 2004